THE JOURNAL OF PHYSICAL CHEMISTRY C
A JOURNAL OF THE AMERICAN CHEMICAL SOCIETY

pubs.acs.org/JPCC

Article

Phase Diagram of Ethane above 300 K

John E. Proctor,* James E. Spender, and Harvey T. Gould

Cite This: J. Phys. Chem. C 2022, 126, 10792−10799

Read Online

ACCESS | Metrics & More | Article Recommendations | Supporting Information

ABSTRACT: We have measured the melting curve of ethane from 300 to 450 K. Our results indicate that to describe all melting curve data above the triple point, it is necessary to account for a kink in the melting curve where the phase III−phase IV solid−solid transition intersects the melting curve. In the solid state, we observe some evidence for a new phase existing close to the melting curve above 300 K. We have observed that the decomposition of ethane at high pressure and temperature can be catalyzed by ruby or samarium-doped yttrium aluminum garnet at a surprisingly low temperature of 375 K.

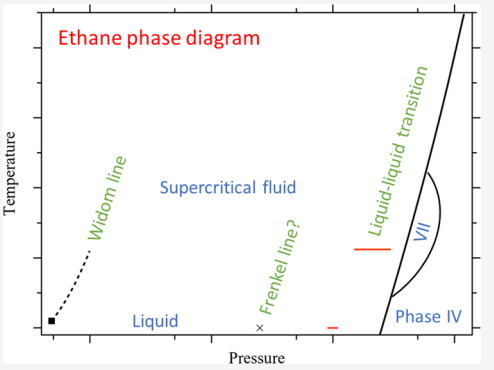

INTRODUCTION

A number of studies exist in the literature concerning the behavior of ethane at high pressure, at ambient temperature,[1−3] and at cryogenic temperatures. The melting curve has been studied up to 33 MPa (96 K) by Straty and Tsumura,[4] to 1 GPa (192 K) by Schutte et al.,[5] and to 2.5 GPa (300 K) by Geijsel et al.[6] Several solid phases (I−III) have been identified up to 200 K,[7] and crystallization at ca. 300 K, 2.5 GPa has been observed into a different phase, phase IV (in ref 8, phase IV is referred to as phase A and phase III is referred to as phase B).[2] A transition from phase IV to phase III has been observed using X-ray diffraction and Raman spectroscopy upon pressure increase at ca. 18 GPa,[3,8] whilst the Frenkel line transition and a second liquid−liquid transition have been observed using Raman spectroscopy in liquid ethane at 300 K, which is just below the critical temperature T_C (305 K).[9]

However, very little is known about ethane above 300 K. A fundamental equation of state (FEOS) is available backed by experimental data to 0.9 GPa and 625 K.[10] Ethane is known to melt at about 2.5 GPa at 300 K and a reasonable extrapolation of the known melting curve from $T \leq 300$ K would lead to melting at 10 GPa, 600 K. The only known study of the melting curve above 300 K is six measurements up to 4.7 GPa, 420 K,[11] which are not in agreement with this extrapolation. To our knowledge, no data exist in the literature on the properties of solid ethane above 300 K or on the properties of fluid ethane above 300 K close to the melting curve.

This lack of data is surprising in view of ethane's importance. It is the simplest molecule containing an sp^3 C−C bond, which is believed to exist in the atmospheres of the outer planets as well as on Titan, and it was recently found to form a clathrate hydrate at 150−173 K.[12] In terms of fundamental physics, it is an excellent "model" system to study recently proposed phenomena in the fluid state at high density such as the Frenkel line. Because the critical temperature of ethane is 305 K, we can access subcritical and near-supercritical temperatures with this system whilst staying reasonably close to ambient temperature to allow the collection of accurate data.

In the present work, we therefore present a body of Raman scattering data on ethane at temperatures up to 450 K and pressures up to 10 GPa. This Raman data allow us to establish the melting curve of ethane above 300 K, as well as to characterize liquid−liquid and solid−solid phase transitions at these conditions.

METHODS

We have conducted eight separate high-temperature Raman spectroscopy experiments. In all cases, pressure was applied using a custom-constructed piston-cylinder diamond anvil cell (DAC) equipped with 600 μm diameter diamond culets. A gasket was prepared for each experiment by indenting 200 μm diameter stainless-steel foil using the DAC before drilling a hole in the center of the indent roughly 300 μm in diameter, using a custom-constructed spark eroder device. The gasket was placed onto the piston diamond anvil, and a crystal of Ruby was placed within the sample chamber to allow pressure measurements using the ruby photoluminescence (PL) method.[13] For the highest temperature experiments (above

Received: February 5, 2022
Revised: June 7, 2022
Published: June 22, 2022

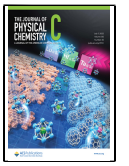

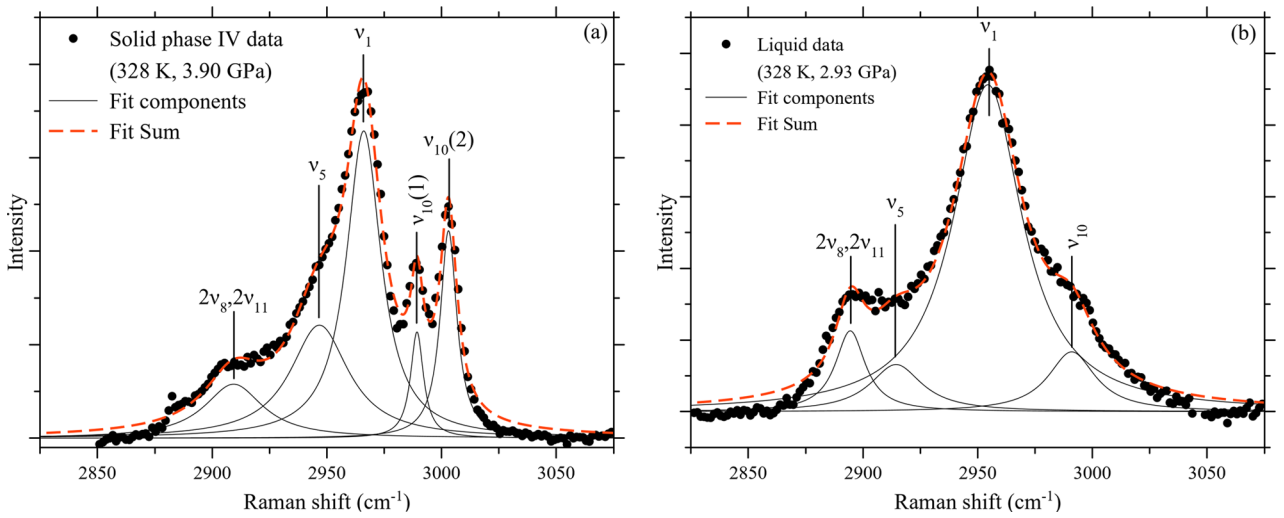

Figure 1. Representative Raman spectra of high-frequency modes in the solid-state phase IV (a) and liquid state (b) at 328 K with Lorentzian fits.

373 K), a crystal of samarium-doped yttrium aluminum garnet (Sm:YAG) was also placed in the sample chamber because the Sm:YAG PL method[14] offers better accuracy than the Ruby fluorescence method at very high temperatures.

As will be discussed later, we observed the decomposition of the ethane sample during some experiments. To verify if this could be catalyzed by the presence of stainless steel, ruby, or Sm:YAG, two additional experiments were performed using rhenium gaskets. In one of these experiments, there was no pressure marker (pressure was instead estimated from the Raman peak because of the stressed diamond anvil[15]), and in the other experiment, Sm:YAG only was utilized as a pressure marker. The melting point obtained in the experiment with no pressure marker has not been utilized in our analysis.

Ethane was loaded cryogenically using the same procedure and apparatus as those in our earlier work on ethane[3,9] and methane.[7,12] We checked that nitrogen contamination was not present by checking for the intense Raman-active vibron from nitrogen at ca. 2300 cm^{-1} after loading.

Raman spectra from ethane and PL spectra from Ruby and Sm:YAG were collected on a single grating spectrometer with 1200 lines/mm and a spectral resolution of 3.25 cm^{-1} half width half maximum (HWHM). A 532 nm laser with a spot size of ca. 1 μm was used to excite Raman scattering and ruby PL, and a 405 nm laser diode was used to excite the Sm:YAG PL as using 532 nm excitation for this results in a overlap between the PL spectrum and the diamond Raman peaks. Raman scattering and PL were both excited using the 180° backscattering geometry.

The DAC was heated using a resistive heater (Watlow) clamped round the outside of the cell. Temperature was measured using a thermocouple mounted close to the diamond. The temperature was held constant to ±2 K whilst data were collected using a custom-constructed temperature controller. Temperature at the thermocouple was measured to a precision of ±0.1 K at T < 473 K and to ±1 K at higher temperatures; however, in reality, some small variation in temperature between the thermocouple and the sample is expected, so ±1 K is a more reasonable estimate of the error in temperature measurement throughout.

Raman spectra were collected upon (a) pressure change at constant temperature and (b) temperature change at approximately constant pressure. Method (a) generally leads to smaller errors because the temperature controller ensures that temperature is held constant whilst the pressure is changed, whereas in case (b), it is unavoidable that pressure will also change when temperature is changed. We therefore used method (a) to diagnose melting in all cases.

The recognized scale for pressure measurement using ruby assumes that the shift in the PL peak position due to the combined effect of pressure and temperature is a linear combination of the separate pressure and temperature effects. In case (a), we calculated pressure by comparison of the ruby PL at high pressure and temperature (P,T) to PL from the same crystal of ruby at ambient pressure, at the temperature at which the experiment was conducted. It was therefore not necessary to explicitly apply the temperature correction. In case (b), pressure was calculated by comparison to a spectrum at ambient pressure and temperature, so the temperature correction did have to be applied explicitly.

The recognized scale for pressure measurement using Sm:YAG assumes that the PL peak positions are independent of temperature. Our own measurements of Sm:YAG PL at high temperature and ambient pressure indicate that the error introduced by this assumption (compared to the linear shift assumption in the ruby scale) is at most ±0.04 GPa. Nonetheless, when measuring pressure in case (a), the pressure was calculated from comparison to the Sm:YAG spectrum at ambient pressure at the temperature at which the experiment was conducted to eliminate this potential error. In case (b), pressure was calculated by comparison to a Sm:YAG spectrum at ambient P,T, and we did not apply any temperature correction to the pressure measurement.

There is no recognized temperature correction to our knowledge for the pressure estimation using the Raman signal from the stressed diamond anvil.[15] However, we observed that upon temperature increase, the Raman signal from the unstressed part of the diamond (i.e., the back of the diamond) shifts to a significantly lower wavenumber upon temperature increase. We therefore estimated pressure by comparing the peak position of the stressed diamond anvil to the unstressed peak position at the same temperature.

Calibration of the Raman spectra was checked using the intense peak at 1332 cm^{-1} from diamond at ambient conditions. All spectral peak positions and widths were

https://doi.org/10.1021/acs.jpcc.2c00875
J. Phys. Chem. C 2022, 126, 10792−10799

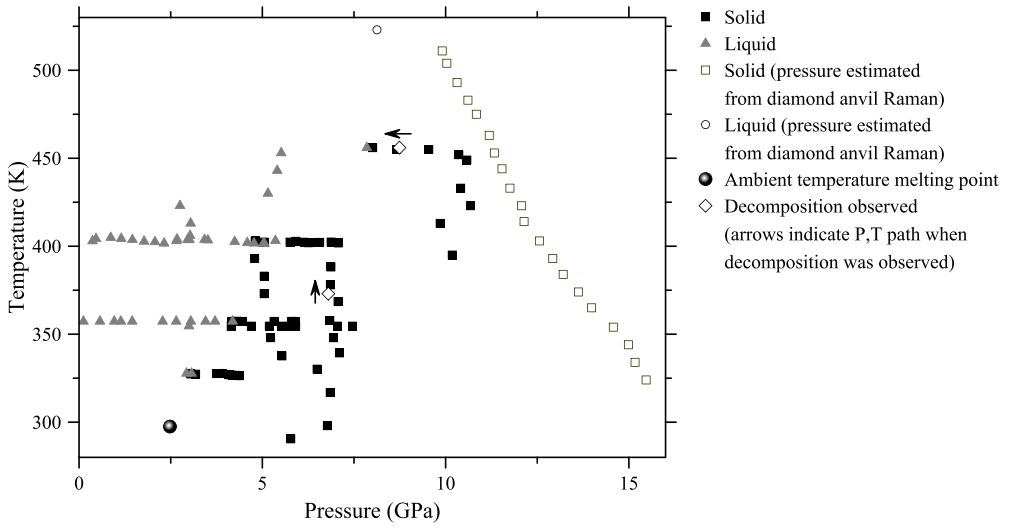

Figure 2. *P,T* points at which Raman data were collected, indicating ethane in the solid and liquid states (squares), melting point at ambient temperature (circle), and *P,T* points where decomposition was observed (diamonds). Arrows indicate the direction of *P,T* change when decomposition was observed.

obtained by fitting Lorentzian peaks in Magicplot Pro after subtraction of a linear baseline.

Liquid and solid ethane have relatively complex Raman spectra, described in detail in publications by ourselves and by other authors.[3,8,9] For the diagnosis of melting, we focused on the overlapping group of C−H stretch and deformation modes around 3000 cm^{-1} as these peaks were found to exhibit a clear qualitative change upon melting at 300 K in earlier studies.[1,3] In all solid phases, the ν_{10} peak (the highest frequency mode) splits into two components. This is not the case in the liquid state. Figure 1 shows representative Raman spectra for this region taken in phase IV of the solid state (a) and in the liquid state (b) at 327 K. Fits and mode assignments are included. We previously showed a similar comparison at 300 K (see the Supporting Information to ref 3). The only peak here we have not fitted is the very weak peak at 2800 cm^{-1} shown in Figure 1a. Because of the weakness of the peak, the fit would be poorly constrained, and the peak does not appear in a sufficiently frequent and reproducible manner to justify fitting.

In our experiments, at 357 and 402 K, we checked the diagnosis of crystallization from the splitting in the ν_{10} mode against the alternate criterion of the splitting of the ν_{11} mode upon crystallization. Both these criteria have been calibrated against visual observation of the solid−liquid equilibrium at 300 K.[1,2] In addition (see Figure 2), at 357 and 402 K, we collected closely spaced data points in the fluid state right from the melting point to GPa. This served as an additional check that the spectral changes we attribute to melting at all temperatures are attributed correctly and were not due instead to a solid−solid phase transition. If this was the case, we would have observed additional changes at lower pressure when melting took place. This did not occur. We observed no substantive changes in the Raman spectra until the liquid−liquid phase transition (which is clearly not first-order) was encountered at pressures far below any reasonable extrapolation of the melting curve.

RESULTS

Melting was diagnosed according to the criterion described earlier, in several experiments where the pressure was varied at constant temperature. From our data above 300 K, and the range of values available in the literature at ca. 300 K, we have identified 5 *P,T* points appropriate to consider as melting points going forward. At ca. 300 K, the melting point has been measured as 2.5 GPa (300 K) by Shimizu et al.,[1] 2.46 GPa (295 K) by Podsiadlo et al.,[2] and 2.7 GPa by Stavrou et al.[8] Because the measurement by Stavrou et al. is an outlier, we have taken the average of the other two values. In our experiment, at 456 K, we took the average pressure of the highest pressure liquid and lowest pressure solid datapoints. However, in our experiments, at 328, 357, and 402 K, more than one pass over the melting point was made, and the highest pressure liquid datapoint actually lay at higher pressure than the lowest pressure solid datapoint. It is possible that this is due to some hysteresis in the melting curve; however, because the errors in pressure measurement at high temperature are hard to quantify, we cannot state with confidence that we have uncovered evidence for hysteresis. We have therefore designated melting as the average pressure of the highest pressure liquid and lowest pressure solid datapoints, the same as that at 456 K. The errors in melting pressure given are obtained from the pressure gap between the highest pressure liquid and lowest pressure solid datapoints. The melting points are summarized in Table 1.

In several experiments, we observed the decomposition of the ethane sample into products that were transparent but had no measurable Raman spectrum. This decomposition was not accompanied by a significant loss of pressure. We have verified that neither pressure decrease at constant temperature nor

Table 1. Melting Points Determined from the Literature[1,2] (at 297.5 K) and in the Present Work (at T > 300 K)

pressure (GPa)	error in pressure (GPa)	temperature (K)	error in temperature (K)
2.48	0.02	297.5	2.5
3.06	0.01	328	1
4.175	0.015	357	1
5.2	0.15	402	1
7.93	0.08	456	1

https://doi.org/10.1021/acs.jpcc.2c00875
J. Phys. Chem. C 2022, 126, 10792−10799

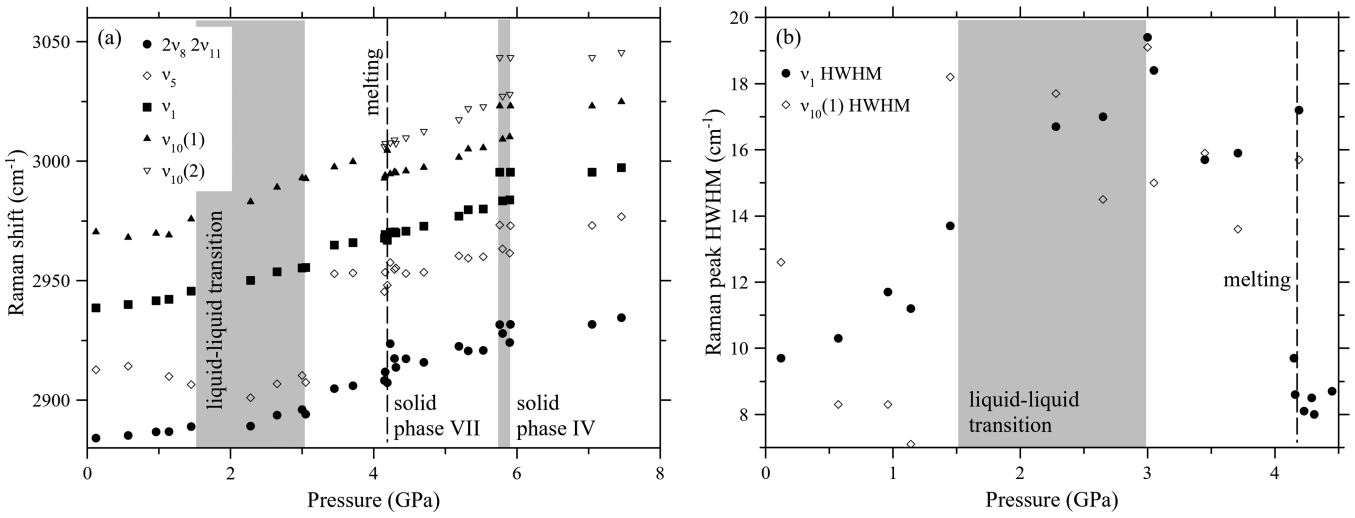

Figure 3. Panel (a) Raman peak position of Raman modes near 3000 cm^{-1} as a function of pressure at 357 K in the liquid and solid states. (b) Widths of principal peaks in this group in the liquid state.

temperature decrease at constant pressure led to the recovery of the ethane Raman spectrum. Because it seemed likely that this decomposition must be catalyzed by something within the sample chamber, we ran additional experiments with a rhenium gasket and Sm:YAG only as a pressure marker and with a rhenium gasket and no pressure marker. The experiment with no pressure marker was the only experiment in which ethane remained stable above about 425 K. Figure 2 shows all *P,T* points at which Raman spectra were collected in our study, an indication of whether the sample was in the solid or the liquid state, and the recognized melting point at 297.5 K. Although all experiments described here took place above ethane's critical temperature of 305 K, we shall use the term "liquid" to describe the sample following melting. This is appropriate because the density and dynamic properties, of the fluid in the *P,T* regime studied are more similar to a rigid liquid than to a gas. *P,T* points at which the decomposition of the sample was observed are also shown, for the cases where the *P,T* at which decomposition took place could be accurately measured.

The trends in the Raman peak position, width (half width half maximum—HWHM), and integrated intensity as a function of pressure were fitted and tracked in our experiments varying pressure at constant temperature in the liquid and solid states. The intensity data in the solid state were not reproducible. This is most likely due to the sample not being a good powder: At high temperature close to the melting curve (especially when making multiple passes over the melting curve), it is likely that the sample consists of a small number of single crystals, so the measured intensity depends on the orientation of these crystals relative to the beam, rather than being a reliable indicator of the spherically averaged Raman scattering cross-section for each mode.

The intensity data in the liquid state were too noisy to observe any clear trends; however, the position and width data in the liquid state indicate in some cases a relatively narrow transition to be observed at ca. 2 GPa. Figure 3 shows representative data of the changes in the Raman peak behavior at the transition, at melting, and at the phase IV—phase VII solid—solid phase transition, which will be discussed later.

In the solid state, we observe a transition evidenced by a sudden jump of ca. 10 cm^{-1} in the Raman peak positions of the group of peaks at 3000 cm^{-1}, occurring at pressures 1—2 GPa above the melting point. It is, however, a separate transition from melting, as evidenced in the example spectra in Figure 4.

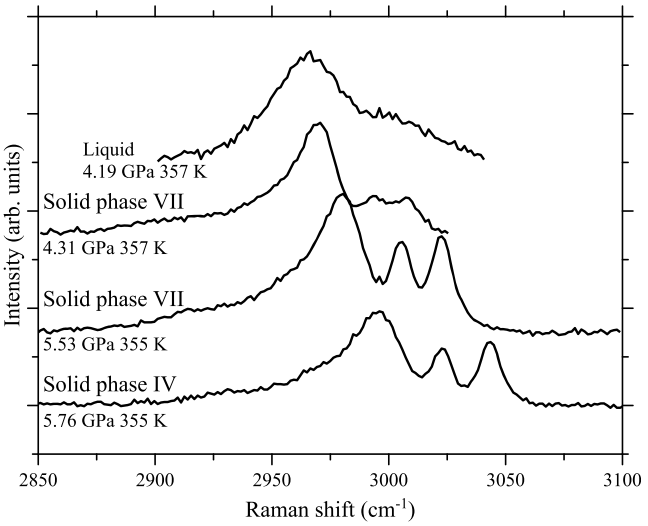

Figure 4. Raman spectra at ca. 355 K from solid phases IV and VII, and the liquid state.

Figure 3a shows the transition in the trend of the Raman peak position versus pressure, showing this jump. We observed this in our experiments at 327 and 355 K but not at higher temperatures.

Even in the solid-state phase IV, we observe two other minor changes in the Raman spectra at $T > 300$ K compared to previous studies at ca. 300 K. We observed the $2\nu_6$ and $2\nu_2$ peaks at ca. 2800 cm^{-1} in the solid state, whereas at ca. 300 K, these were only observed in the liquid state.[9] However the peaks are very weak in any case, so we cannot state that their lack of observation in the solid state at ca. 300 K is conclusive evidence of absence. Similarly, in the current work, we found it necessary to include the ν_5 at ca. 2925 cm^{-1} in our fits for the solid state, which was only required in the liquid state at ca. 300 K. However, because the peak is simply a weak shoulder on the intense ν_1 peak in any case, the fact it was not necessary

https://doi.org/10.1021/acs.jpcc.2c00875
J. Phys. Chem. C 2022, 126, 10792—10799

to fit it in the solid state at ca. 300 K is not conclusive evidence of absence.

DISCUSSION

Melting. Our results enable us to construct a melting curve for ethane and examine the degree to which the different melting point measurements in the literature are consistent with each other, and with our results. In Figure 5, we plot the

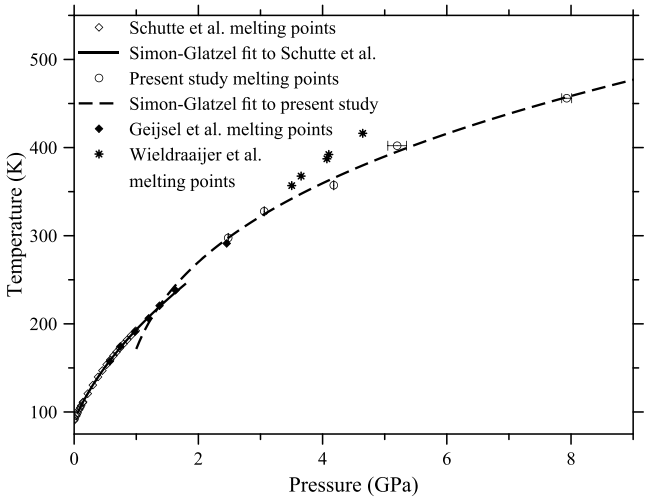

Figure 5. Melting curve datapoints from phase III and from phase IV with Simon−Glatzel fit parameters to both datasets. Error bars are shown when larger than the datapoints. The datapoint from Wieldaaijer et al. at 328 K lies very close to our own datapoint, so it has been omitted for clarity.

melting points obtained in the present study, along with those from relevant previous studies. The principal existing work on the melting curve is that of Schutte et al.,[5] in which tabulated melting points are given up to ca. 1 GPa (192 K). The gap between here and the recognized melting point at ca. 300 K is covered by Geijsel et al.;[6] however, only a graphical representation of their data is available. We have extracted the melting points from the graph for reproduction in Figure 5.

Above 300 K, the data of Wieldraaijer et al.[11] are also available only in the graphical form, and we have extracted these data also for presentation in Figure 5, even though they are clearly not consistent with our own data, or a reasonable extrapolation of curves fitted to the data in refs 5, 6. We have omitted the data of Straty and Tsumura (ref 4) because of the small range covered by the dataset (up to 33 MPa). The extracted data from refs 6, 11 are given in the Supporting Information.

In the P,T range covered by the melting curve data in Figure 5, several solid−solid phase transitions intersect the melting curve. In principle, each of these could lead to a kink in the melting curve because of the Clausius−Clapeyron rule. In reality, two fits utilizing the Simon−Glatzel equation (eq 1) are sufficient to reproduce all data with reasonable accuracy. The Simon−Glatzel equation is constrained to pass through a specific P,T point P_0, T_0 regardless of the values of the adjustable parameters a and b. We have therefore fitted the melting data of ref 5 with a Simon−Glatzel equation constrained to pass through the triple point, and the melting data from the present work with a Simon−Glatzel equation constrained to pass through the melting point from Table 1 at 300 K. We have not fitted to the data from ref 6 or 11 because tabulated data from these studies are not available, and the data from ref 11 are not consistent with our own data. Various reasons for the discrepancy between ref 11 and our data are given in the Supporting Information, and our Simon-Glatzel fit parameters are given in Table 2.

$$T = T_0\left(1 + \frac{P - P_0}{a}\right)^{1/b} \quad (1)$$

Table 2. Fit Parameters for Simon−Glatzel Melting Curve Fits Shown in Figure 5

data	P_0 (GPa)	T_0 (K)	a (GPa)	b
Ref 5.	1.14×10^{-9}	90.368	0.270 ± 0.003	2.0358 ± 0.01
Present work	2.48	297.500	1.7728 ± 0.6	3.269 ± 0.7

Liquid−Liquid Phase Transitions. In our earlier work on ethane in the subcritical regime at 300 K ($0.98T_C$),[9] we identified the Frenkel line at ca. 250 MPa, followed by a liquid−liquid phase transition at ca. 1000 MPa. At high temperature, pressure is much harder to control. The errors in pressure measurement and fluctuations in pressure are unavoidably greater (and hard to quantify). As a result, we do not have an adequate number of data points below 0.5 GPa to detect the presence or otherwise of any transitions at these very low pressures. At 400 K, the amount of scatter in the data is such that we also cannot detect the presence or absence of any liquid−liquid phase transition. We are, however, able to identify a liquid−liquid phase transition at ca. 355 K (albeit with a lower level of confidence than in our earlier work at 300 K).

The transition (as shown in the example data in Figure 3 and in other data in the Supporting Information) takes place at 1.5−3 GPa. While the changes observed are those characteristic of a transition from behavior which is less similar to that of a gas, and more similar to that of a dense liquid, the high transition pressure means that it is unlikely to be the Frenkel line. Extrapolation of available PVT data from lower pressures using the Xiang-Deiters EOS[16] (implemented using the ThermoC code[17]) indicates that the density at 356 K ($1.17T_C$), 2 GPa is ca. 0.026 Mol./cm^3, whilst the density when the Frenkel line is crossed at 300 K ($0.98T_C$), 250 MPa is 0.020 Mol./cm^3. It seems unlikely for the density at which the Frenkel line is crossed to increase by 30% during such a small temperature increase. It would certainly be at odds with the findings of both theoretical and experimental investigations into the Frenkel line in a variety of atomic and molecular fluids (reviewed in refs 18, 19).

The transition observed is therefore most likely to be the same transition as the liquid−liquid phase transition we observed previously[9] at ca. 1 GPa, 300 K. However, whilst the changes in the Raman peak behavior at 1.5−3 GPa are similar to those we observed at ca. 1 GPa, 300 K in our earlier work, they are not identical, so we cannot assign them to the same transition with complete confidence.

Solid−Solid Transition. In our experiments, at constant temperatures of 328 and 357 K, we observe a discontinuous change in the Raman spectra that would seem to indicate a transition between two solid phases at pressures not far above the melting point. The transition to the new phase involves a sudden jump in the peak positions of the group of high

https://doi.org/10.1021/acs.jpcc.2c00875
J. Phys. Chem. C 2022, 126, 10792−10799

frequency modes at ca. 3000 cm^{-1} but negligible effect on the other modes. This phenomenon has not been observed in any of the phase transitions at 300 K, either by ourselves[3] or by other authors. We will therefore label this new phase as phase VII (phases—or potential phases - I to VI have already been described in ref 3 and refs therein). Table 3 lists (at each temperature) the lowest pressure at which phase IV was observed, the highest pressure at which phase VII was observed, and the transition pressure obtained from the average of these two. At 328 K, the transition lies very close to the melting point. At 354.6 K, the highest pressure at which phase VII was observed was slightly higher than the lowest pressure at which phase IV was observed. However, given the difficulty in quantifying all errors in pressure measurement, we do not consider this to be convincing evidence for any hysteresis in the transition. These transition pressures are indicated later on the phase diagram in Figure 6.

Table 3. Transition Pressures for Phase IV—Phase VII Transition

temperature (K)	lowest phase IV pressure (GPa)	highest phase VII pressure (GPa)	transition pressure (GPa)
328	3.18	3.05	3.12 ± 0.07
354.6	5.76	5.90	5.83 ± 0.07

CONCLUSIONS

The measurements made in the present work, combined with earlier studies as cited, allow us to present the phase diagram of ethane shown in Figure 6. To extend the measurement of the melting curve to higher *P,T*, it will be necessary to switch to alternate methods of pressure measurement because of our observation that both ruby and Sm:YAG catalyze some reaction involving the ethane. X-ray diffraction from a transition metal pressure marker is one possibility, although this may not solve the problem. Transition metals are used in industry and science to catalyze the decomposition of hydrocarbons (at ambient or low pressure, for instance, in chemical vapor deposition growth of graphene[20]), and it has been speculated that this may also take place at high pressure when transition metal absorbers are used in laser heating experiments on hydrocarbons.[21]

Our results suggest that it will be necessary to look in detail at the need for temperature correction to the diamond anvil Raman pressure estimation method. If we do not apply the temperature correction proposed earlier in the Methods section, we obtain pressures at ca. 500 K that are about 2 GPa lower than what we have presented above. This would imply melting taking place at a significantly lower pressure than at 457 K. In fact, extrapolation of our Simon—Glatzel fit to the melting data predicts melting at 12 GPa, 524 K. Whilst the diamond anvil Raman pressure gauge has been tested against the ruby scale at 300 K in many laboratories (including our own[3,22]), there is clearly a need to have a careful look at what temperature correction may be required, and to test it directly against the Sm:YAG pressure scale at $T \geq 300$ K. This is especially true because pressure measurement at high temperature is one of the two principal applications of the diamond anvil Raman gauge (along with pressure measurement at megabar pressures).

Our data indicate that a new phase (phase VII) exists close to the melting curve above 300 K. While it is difficult to see how such a large (~10 cm^{-1}) jump in the Raman frequencies of some peaks can occur, repeated in several experiments, in the absence of a structural phase transition, the existence of this phase needs to be verified using X-ray or (preferably) neutron diffraction. Raman spectroscopy alone cannot generally be considered conclusive evidence of structural phase transition. If phase VII is real, then at some point between 300 and 325 K, there is a triple point between the phase IV—phase VII phase boundary and the melting curve, where another kink in the melting curve could exist. The fact that a single Simon—Glatzel equation gives good agreement with the melting data for all phase IV—liquid and phase VII—liquid transitions measured in the present and previous work[6] shows (via the Clausius—Clapeyron rule) that the volume change and latent heat of melting are similar from both phases. Further evidence for this conclusion is that the ν_3 C—C stretching mode (which undergoes a large jump on melting) is barely affected by the phase IV—phase VII transition (see the Supporting Information). We would expect a significant jump

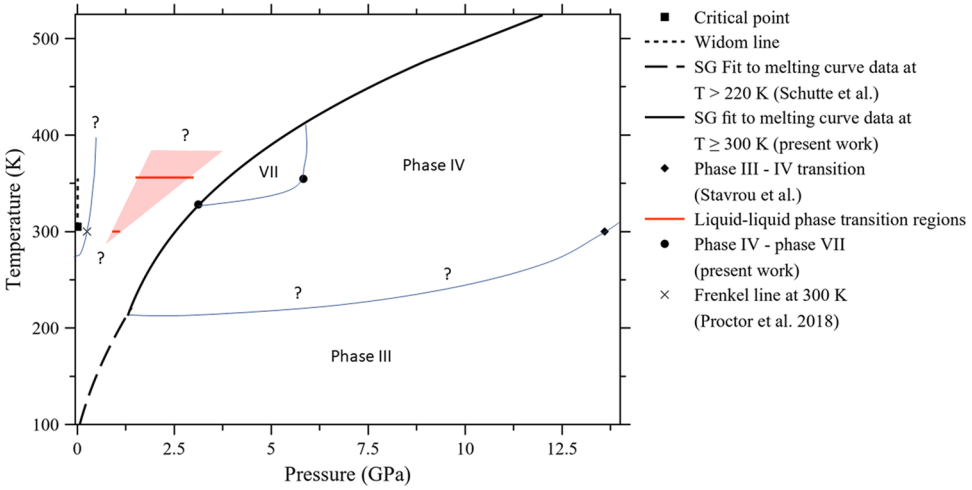

Figure 6. Phase diagram of ethane. Thick lines are obtained directly from experimental data, thin lines are a guide to the eye without physical significance. The low temperature phases I and II have been omitted for clarity.

https://doi.org/10.1021/acs.jpcc.2c00875
J. Phys. Chem. C 2022, 126, 10792—10799

in the frequency of this Raman mode if the transition involved a significant volume change.

Chemical changes in hydrocarbons under high pressure−high temperature conditions have been observed in a number of previous studies on methane and ethane,[21,23] as well as propane,[24] including reactions to products with no measurable Raman spectrum. For instance, as shown in ref 25, benzene was compressed at 300 K, and no measurable Raman spectrum was observed above 43 GPa. In our laboratory, we conducted an (unpublished) experiment verifying this. We observed that even after complete pressure release, no Raman spectrum was observed. Therefore, the observation of the decomposition of ethane to products with no measurable Raman spectrum is not surprising.

What is surprising is the very low temperature required for the decomposition. In other cases to our knowledge, temperatures above 1500 K (obtained using laser heating) have been required. The fact that the reaction could be avoided (in the present work) by conducting the experiment with a rhenium gasket (instead of stainless steel) and no pressure marker indicates that it is not an underlying property of ethane, merely an anomaly due to the right (wrong) materials being present inside the sample chamber. Nevertheless, the present results do serve as a warning about the need for extreme care to study the catalytic effect of any additional materials on the sample chamber during the experiment.

Whilst Raman spectroscopy experiments at high pressure and high temperature in the DAC have taken place for decades, the use of molecular dynamics (MD) simulations to directly predict the changes in fluid Raman spectra as a function of pressure and temperature is still in its infancy.[26,27] The present study provides a large amount of high-temperature Raman data, which can be used to test MD simulations. These data are available on request.

■ ASSOCIATED CONTENT

Supporting Information

The Supporting Information is available free of charge at https://pubs.acs.org/doi/10.1021/acs.jpcc.2c00875.

Tabulated melting curve data from previous studies, data demonstrating other changes on liquid−liquid transition at 1.5−3 GPa, graphs showing the C−C ν_3 stretching mode on melting, and phase IV−VII transition at 357 K (PDF)

■ AUTHOR INFORMATION

Corresponding Author

John E. Proctor − *Materials and Physics Research Group, School of Science, Engineering and Environment, University of Salford, Manchester M5 4WT, U.K.;* orcid.org/0000-0003-3639-8295; Email: j.e.proctor@salford.ac.uk

Authors

James E. Spender − *Materials and Physics Research Group, School of Science, Engineering and Environment, University of Salford, Manchester M5 4WT, U.K.*

Harvey T. Gould − *Materials and Physics Research Group, School of Science, Engineering and Environment, University of Salford, Manchester M5 4WT, U.K.*

Complete contact information is available at: https://pubs.acs.org/10.1021/acs.jpcc.2c00875

Notes

The authors declare no competing financial interest.

■ ACKNOWLEDGMENTS

We would like to acknowledge useful discussions with Dr. Helen Maynard-Casely, Dr. John Loveday, and Dr. Ciprian Pruteanu.

■ REFERENCES

(1) Shimizu, H.; Shimazaki, I.; Sasaki, S. High-Pressure Raman Study of Liquid and Molecular Crystal Ethane Up to 8 GPa. *Jpn. J. Appl. Phys.* **1989**, *28*, 1632−1635.

(2) Podsiadlo, M.; Olejniczak, A.; Katrusiak, A. A New Ethane Polymorph. *Cryst. Growth Des.* **2017**, *17*, 228−232.

(3) Read, L. Q.; Spender, J. E.; Proctor, J. E. Raman Spectroscopy of Ethane (C_2H_6) to 120 GPa at 300 K. *J. Raman Spectrosc.* **2020**, *51*, 2311.

(4) Straty, G. C.; Tsumura, R. Phase Transition and Melting Pressures of Solid Ethane. *J. Chem. Phys.* **1976**, *64*, 859−861.

(5) Schutte, M. H. M.; Prins, K. O.; Trappeniers, N. J. Nuclear Magnetic Resonance in Solid Ethane at High Pressure. *Phys. B* **1987**, *144*, 357−367.

(6) Geijsel, J. I.; Schouten, J. A.; Trappeniers, N. J. *The Phase Diagram of Ethane Under High Pressure.* In *Proceedings of the VIIth International AIRAPT Conference (Organised Jointly with the EHPRG)*; Pergamon Press, 1980; pp. 645−647.

(7) Klimenko, N. A.; Gal'tsov, N. N.; Prokhvatilov, A. I. Structure, Phase Transitions, and Thermal Expansion of Ethane C_2H_6. *Low Temp. Phys.* **2008**, *34*, 1038−1043.

(8) Stavrou, E.; Maryewski, A. A.; Lobanov, S. S.; Oganov, A. R.; Konôpková, Z.; Prakapenka, V. B.; Goncharov, A. F. Ethane and Methane at High Pressures: Structure and Stability. *J. Chem. Phys.* **2021**, *155*, No. 184503.

(9) Proctor, J. E.; Bailey, M.; Morrison, I.; Hakeem, M. A.; Crowe, I. F. Observation of Liquid−Liquid Phase Transitions in Ethane at 300 K. *J. Phys. Chem. B* **2018**, *122*, 10172−10178.

(10) Bücker, D.; Wagner, W. A Reference Equation of State for the Thermodynamic Properties of Ethane for Temperatures from the Melting Line to 675 K and Pressures up to 900 MPa. *J. Phys. Chem. Ref. Data* **2006**, *35*, 205.

(11) Wieldraaijer, H.; Schouten, J. A.; Trappeniers, N. J. Investigation of the Phase Diagrams of Ethane, Ethylene, and Methane at High Pressures. *High Temp.-High Press.* **1983**, *15*, 87.

(12) Vu, T. H.; Choukroun, M.; Sotin, C.; Muñoz-Iglesias, V.; Maynard-Casely, H. E. Rapid Formation of Clathrate Hydrate From Liquid Ethane and Water Ice on Titan. *Geophys. Res. Lett.* **2020**, *47*, No. e2019GL086265.

(13) Shen, G.; Wang, Y.; Dewaele, A.; Wu, C.; Fratanduo, D. E.; Eggert, J.; Klotz, S.; Dziubek, K. F.; Loubeyre, P.; et al. Toward an International Practical Pressure Scale: A Proposal for an IPPS Ruby Gauge (IPPS-Ruby2020). *High Press Res.* **2020**, *40*, 299−314.

(14) Trots, D. M.; Kurnosov, A.; Ballaran, T. B.; Tkachev, S.; Zhuravlev, K.; Prakapenka, V.; Berkowski, M.; Frost, D. J. The Sm:YAG Primary Fluorescence Pressure Scale. *J. Geophys. Res.: Solid Earth* **2013**, *118*, 5805−5813.

(15) Akahama, Y.; Kawamura, H. Pressure Calibration of Diamond Anvil Raman Gauge to 310 GPa. *J. Appl. Phys.* **2006**, *100*, No. 043516.

(16) Xiang, H. W.; Deiters, U. K. A New Generalized Corresponding-states Equation of State for the Extension of the Lee−Kesler Equation to Fluids Consisting of Polar and Larger Nonpolar Molecules. *Chem. Eng. Sci.* **2008**, *63*, 1490.

(17) Deiters, U. K. ThermoC a modular program package for calculating thermodynamic data (pVT data, caloric data, phase equilibria) of pure fluids as well as fluid mixtures from arbitrary equations of state and mixing rules, http://thermoc.uni-koeln.de/ (accessed 4th January 2022).

(18) Proctor, J. E. *The Liquid and Supercritical Fluid States of Matter*; CRC Press: Boca Raton, 2020.

(19) Cockrell, C.; Brazhkin, V. V.; Trachenko, K. Transition in the Supercritical State of Matter: Review of experimental evidence. *Phys. Rep.* **2021**, *941*, 1−27.
(20) Li, X.; Cai, W.; An, J.; Kim, S.; Nah, J.; Yang, D.; Piner, R.; Velamakanni, A.; Jung, I.; Tutuc, E.; et al. Large-Area Synthesis of High-Quality and Uniform Graphene Films on Copper Foils. *Science* **2009**, *324*, 1312−1314.
(21) Zerr, A.; Serghiou, G.; Boehler, R.; Ross, M. Decomposition of Alkanes at High Pressures and Temperatures. *High Press. Res.* **2006**, *26*, 23.
(22) Proctor, J. E.; Maynard-Casely, H. E.; Hakeem, M. A.; Cantiah, D. Raman Spectroscopy of Methane (CH_4) to 165 GPa: Effect of Structural Changes on Raman Spectra. *J. Raman Spectrosc.* **2017**, *48*, 1777−1782.
(23) Kolesnikov, A.; Kutcherov, V. G.; Goncharov, A. F. Methane-derived Hydrocarbons Produced Under Upper-mantle Conditions. *Nat. Geosci.* **2009**, *2*, 566−570.
(24) Kudryavtsev, D. A.; Fedotenko, T. M.; Koemets, E. G.; Khandarkhaeva, S. E.; Kutcherov, V. G.; Dubrovinski, L. S. Raman Spectroscopy Study on Chemical Transformations of Propane at High Temperatures and High Pressures. *Sci. Rep.* **2020**, *10*, 1483.
(25) Hillier, N. S.; Schilling, J. S. Search for metallization in benzene to 209 GPa pressure. *High Press. Res.* **2014**, *34*, 1.
(26) Hou, R.; Pan, D. Raman Spectra of Hydrocarbons Under Extreme Conditions of Pressure and Temperature: a First-principles Study. *J. Phys. D: Appl. Phys.* **2022**, *55*, No. 044003.
(27) Proctor, E. J.; Pruteanu, C. G.; Morrison, I.; Crowe, I. F.; Loveday, J. S. Transition from Gas-like to Liquid-like Behavior in Supercritical N_2. *J. Phys. Chem. Lett.* **2019**, *10*, 6584−6589.

https://doi.org/10.1021/acs.jpcc.2c00875
J. Phys. Chem. C 2022, 126, 10792−10799